Mahmoud Mashali-Firouzi and Mohammad Maleki*

A multiple-step adaptive pseudospectral method for solving multi-order fractional differential equations

https://doi.org/10.1515/nleng-2018-0079
Received May 23, 2018; revised August 30, 2018; accepted November 6, 2018.

Abstract: The nonlocal nature of the fractional derivative makes the numerical treatment of fractional differential equations expensive in terms of computational accuracy in large domains. This paper presents a new multiple-step adaptive pseudospectral method for solving nonlinear multi-order fractional initial value problems (FIVPs), based on piecewise Legendre–Gauss interpolation. The fractional derivatives are described in the Caputo sense. We derive an adaptive pseudospectral scheme for approximating the fractional derivatives at the shifted Legendre–Gauss collocation points. By choosing a step-size, the original FIVP is replaced with a sequence of FIVPs in subintervals. Then the obtained FIVPs are consecutively reduced to systems of algebraic equations using collocation. Some error estimates are investigated. It is shown that in the present multiple-step pseudospectral method the accuracy of the solution can be improved either by decreasing the step-size or by increasing the number of collocation points within subintervals. The main advantage of the present method is its superior accuracy and suitability for large-domain calculations. Numerical examples are given to demonstrate the validity and high accuracy of the proposed technique.

Keywords: Fractional initial value problem; Caputo derivative; Multiple-step pseudospectral method; Shifted Legendre-Gauss points; Collocation; Error estimates

1 Introduction

Fractional calculus has a long history because, starting from a letter from Leibniz to L'Hospital in 1695, it has been developing up to now. In spite of this long history, only in recent decades fractional calculus and fractional differential equations have found applications in several different disciplines, such as in the fields of Bode's analysis of feedback amplifiers, aerodynamics and polymer rheology, chemistry, engineering, finance and so forth [1–3]. Some natural physics processes and dynamic system processes with memory can be better described by fractional differential equations [4] because the fractional order differential operators are non-local operators. A review of some applications of fractional derivatives in continuum and statistical mechanics is given by Mainardi [5]. In mechanics, for example, fractional derivatives have been successfully used to model damping forces with memory effect or to describe state feedback controllers [6]. In particular, the Bagley–Torvik equation [1, 7, 8] with 1/2-order derivative or 3/2-order derivative describes motion of real physical systems, an immersed plate in a Newtonian fluid and a gas in a fluid, respectively. In addition, almost all systems containing internal damping are not suitable to be described properly by the classical methods, but the fractional calculus represents one of the promising tools to incorporate in a single theory both conservative and nonconservative phenomena [9]. Recently, Tenreiro-Machado [10] investigated a new application of fractional calculus to memristor systems which generalize the notion of electrical elements.

Due to the increasing applications and because of the difficulties in attaining the analytical solutions for most of the fractional differential equations the need for finding efficient computational algorithms for obtaining numerical solutions arises. The numerical solution of fractional differential equations has attached considerable attention from many researchers. During the past decades, an increasing number of numerical schemes are being developed. These methods include finite difference approximation methods [11], collocation methods [12–14], the

***Corresponding Author: Mohammad Maleki,** Department of Mathematics, Faculty of Mohajer, Isfahan Branch, Technical and Vocational University (TVU), Isfahan, Iran, E-mail: mm_maleki2005@yahoo.com
Mahmoud Mashali-Firouzi, Department of Mathematics, Faculty of Mohajer, Isfahan Branch, Technical and Vocational University (TVU), Isfahan, Iran

Adomian decomposition method [15–17], variational iteration method [18], operational matrix methods [19–25], and homotopy method [26, 27]. Kumar and Agrawal [28] presented polynomial approximated methods to a class of fractional differential equation by considering the fact that fractional differential equation can be reduced to Volterra type integral equation. According to quadrature formula approach, Diethelm [29] proposed an implicit algorithm for the approximated solution to an important class of fractional differential equation. Esmaeili et al. [30] utilized the pseudospectral method for solving fractional differential equations. Maleki et al. [31] proposed a single-step adaptive pseudospectral method for solving a class of multi-term fractional boundary value problems. Kazem et al. [32] constructed a general formulation for the fractional-order Legendre functions to obtain the solution of the fractional-order differential equations using the Tau method. Rad et al. [33] presented a numerical solution of fractional differential equations with a Tau method based on Legendre and Bernstein polynomials. Baffet and Hesthaven [34] proposed a kernel compression scheme for solving fractional differential equations.

Pseudospectral or orthogonal collocation methods are efficient and highly accurate techniques for numerical solution of differential equations [35, 36]. The three most commonly used sets of collocation points are Gauss, Gauss–Radau, and Gauss–Lobatto points. They differ significantly in that the Gauss points include neither of the endpoints, the Gauss–Radau points include one of the endpoints, and the Gauss–Lobatto points include both of the endpoints. On bounded domains, pseudospectral methods are usually based on Jacobi and shifted Jacobi polynomials or even nonclassical orthogonal polynomials [37]. The main characteristic behind the approach using this technique is that it reduces a problem to those of solving a system of algebraic equations. Pseudospectral methods can be categorized into global (single-interval) and adaptive (multiple-interval) schemes. Global pseudospectral methods use global polynomials together with Gaussian quadrature collocation points which is known to provide accurate approximations that converge exponentially for problems whose solutions are smooth over the whole domain of interest [35]. On the other hand, adaptive pseudospectral methods increase the utility of pseudospectral methods while attempting to maintain as close to exponential convergence as possible. They allow the number of subintervals, subinterval widths, and polynomial degrees to vary throughout the time interval of interest.

Since a fractional derivative is a non-local operator, it is very natural to consider a global method like the global pseudospectral method for its numerical solution [12]. However, a global pseudospectral method is not suited for large intervals because for ensuring the convergence, the length of interval on which the underlying problems are defined should be limited [38]. On the other hand, in global pseudospectral methods it is not convenient to resolve the corresponding discrete system with very large number of collocation points. To remove this deficiency, adaptive version of pseudospectral method, which is based on the domain decomposition procedure, is considered [38–40]. To the best of our knowledge, adaptive pseudospectral methods are not well studied for solving fractional differential equations.

In the present paper, we propose an efficient multiple-step adaptive pseudospectral method based on shifted Legendre polynomials for the numerical solution of the linear and nonlinear multi-order fractional initial value problems (FIVPs), which involve Caputo fractional derivatives. First, a step-size is considered and then the multi-order FIVP is replaced with a sequence of FIVPs in subintervals, where the initial conditions of the k^{th} FIVP (k^{th} step) are determined using the approximate solution obtained earlier at step $k-1$. By using the Caputo definition, a stable numerical scheme is derived for approximating the fractional derivatives at shifted Legendre–Gauss (ShLG) collocation points. The obtained FIVPs in subintervals are then step by step reduced to systems of algebraic equations using collocation based on the ShLG points. Some error estimates and convergence properties of the proposed method are investigated. The method is demonstrated by several examples of varying complexity and is found to be a viable method for efficiently and accurately solving multi-order FIVPs.

The proposed method has the following advantages: First, in the present method the FIVP is solved step by step, thus, instead of a large scale algebraic system relatively small scale algebraic systems are obtained in subintervals, which greatly reduces the computational complexity and storage requirements. Besides, accurate results can be obtained with a moderate number of collocation points in each subinterval. Second, the present method can be implemented for large-domain calculations. Third, this new algorithm also works well even for some solutions having oscillatory behavior.

The outline of this paper is as follows: We begin by introducing some necessary definitions of the fractional calculus theory and mathematical preliminaries of Legendre polynomials which are required for our subsequent development. In Section 3, the statement of the problem is presented. Section 4 is devoted to explanation of the proposed method and some error estimates. In Section 5, we report our numerical findings and demonstrate the accuracy and validity of the proposed method. Finally, in Section 6 we provide conclusions.

2 Preliminaries

2.1 Definitions of fractional derivatives

In this subsection, we start by recalling the essential definitions of the fractional calculus. There are various definitions related to fractional integration and differentiation, such as Grünwald–Letnikov's definition, Riemann–Liouville's definition and Caputo definition [1]. Suppose $\alpha > 0$, $n = [\alpha] + 1$, where $[\alpha]$ denotes the integer part of α, and the function $f(x)$ has n continuous bounded derivatives in $[0, T]$, $f \in \mathrm{C}^n[0, T]$, for every $T > 0$.

Definition 1. The Riemann–Liouville fractional derivative of order $\alpha > 0$ is defined by

$$\mathfrak{D}^\alpha f(x) = \left(\frac{\mathrm{d}}{\mathrm{d}x}\right)^n \frac{1}{\Gamma(n-\alpha)} \int_0^x \frac{f(t)}{(x-t)^{\alpha+1-n}}\,\mathrm{d}t. \tag{2.1}$$

Definition 2. The Caputo derivative of fractional order $\alpha > 0$ is defined as

$$D^\alpha f(x) = \frac{1}{\Gamma(n-\alpha)} \int_0^x \frac{f^{(n)}(t)}{(x-t)^{\alpha+1-n}}\,\mathrm{d}t. \tag{2.2}$$

Recall that for $\alpha \in \mathbb{N}$ ($\mathbb{N} = \{1, 2, \dots\}$), the Caputo differential operator coincides with the usual differential operator of an integer order. Further, it is seen that fractional differential operators are defined through convolution integrals. Therefore, unlike integer order derivatives, they are nonlocal operators. They depend on all function values from its lower limit $t = 0$ up to the evaluation point $t = x$. This characteristic makes their evaluation more complicated.

Recalling the fact that the Grünwald–Letnikov definition coincides with the Riemann–Liouville derivative, it is pointed out that the Riemann–Liouville derivative has certain disadvantages when trying to model real-world phenomena with fractional differential equations [41]. Therefore, we shall use a modified fractional differential operator D^α proposed by Caputo in his work on the theory of viscoelasticity [42]. The reason for adopting the Caputo definition is as follows: in order to produce a unique solution for differential equations, it is required to specify additional conditions. For the case of differential equations with the Caputo derivatives, these additional conditions are just the traditional conditions, which are akin to those of classical differential equations. In contrast, for differential equations with the Riemann-Liouville derivatives, we are forced to specify some fractional derivatives of the unknown solution at the initial point $x = 0$, which are functions of x. In practical applications, these initial values are frequently not available, and it may not even be clear what their physical meaning is (see [43]). For more details about the mathematical properties of fractional derivatives, see [1–4].

2.2 Basic properties of Legendre and shifted Legendre polynomials

The well-known Legendre polynomials, $P_i(z)$, $i = 0, 1, \dots,$ can be determined by the following recurrence relation:

$$P_{i+1}(z) = \frac{2i+1}{i+1} z P_i(z) - \frac{i}{i+1} P_{i-1}(z), \quad i = 1, 2, \dots, \tag{2.3}$$

where $P_0(z) = 1$ and $P_1(z) = z$. If $P_i(z)$ is normalized so that $P_i(1) = 1$, then for any i, the Legendre polynomials in terms of power of z are

$$P_i(z) = \frac{1}{2^i} \sum_{k=0}^{[\frac{i}{2}]} (-1)^k \binom{i}{k} \binom{2i-2k}{i} z^{i-2k},$$

where $\left[\frac{i}{2}\right]$ denotes the integer part of $\frac{i}{2}$. Also, they are orthogonal with respect to L^2 inner product on the interval $[-1, 1]$ with the weight function $w(z) = 1$, that is

$$\int_{-1}^{1} P_i(z) P_j(z)\,\mathrm{d}z = \frac{2}{2i+1}\delta_{ij},$$

where δ_{ij} is the Kronecker delta. The Legendre–Gauss (LG) collocation points $-1 < z_1 < z_2 < \dots < z_{N-1} < 1$ are the roots of $P_{N-1}(z)$. There are no explicit formulas for the LG points; however, they can be computed numerically using existing subroutines. The LG points have the property that

$$\int_{-1}^{1} p(z)\,\mathrm{d}z = \sum_{j=1}^{N-1} w_j p(z_j),$$

is exact for polynomials of degree at most $2N - 3$, where

$$w_j = \frac{2}{(1 - z_j^2)[P'_{N-1}(z_j)]^2}, \quad j = 1, 2, \dots, N-1, \tag{2.4}$$

are the LG quadrature weights. For more details about Legendre polynomials, see [35].

The shifted Legendre polynomials on the interval $x \in [a, b]$ are defined by

$$\widehat{P}_i(x) = P_i\left(\frac{1}{b-a}(2x - a - b)\right), \quad i = 0, 1, 2, \dots,$$

which are obtained by an affine transformation from the Legendre polynomials. The set of shifted Legendre polynomials is a complete $L^2(a,b)$-orthogonal system with the weight function $w(x) = 1$. Thus, any function $f \in L^2(a,b)$ can be expanded in terms of shifted Legendre polynomials. The shifted Legendre–Gauss (ShLG) collocation points $a < x_1 < x_2 < \ldots < x_{N-1} < b$ on the interval $[a,b]$, are obtained by shifting the LG points, z_j, using the transformation

$$x_j = \frac{1}{2}\left((b-a)z_j + a + b\right), \quad j = 1, 2, \ldots, N-1. \qquad (2.5)$$

Thanks to the property of the standard LG quadrature, it follows that for any polynomial p of degree at most $2N-3$ on (a,b),

$$\begin{aligned}\int_a^b p(x)\,\mathrm{d}x &= \frac{b-a}{2}\int_{-1}^{1} p\left(\frac{1}{2}\left((b-a)z + a + b\right)\right)\mathrm{d}z \\ &= \frac{b-a}{2}\sum_{j=1}^{N-1} w_j p\left(\frac{1}{2}\left((b-a)z_j + a + b\right)\right) \\ &= \sum_{j=1}^{N-1} \widehat{w}_j p(x_j), \qquad (2.6)\end{aligned}$$

where $\widehat{w}_j = \frac{b-a}{2}w_j$, $1 \le j \le N-1$ are the ShLG quadrature weights.

3 Problem statement

Consider the IVP of multi-order fractional differential equation

$$D^{\nu}y(x) = F\left(x, y(x), D^{\alpha_1}y(x), \ldots, D^{\alpha_m}y(x)\right), \quad x \ge 0, \qquad (3.1)$$

with initial conditions

$$y^{(r)}(0) = d_r, \quad r = 0, 1, \ldots, l-1, \qquad (3.2)$$

where $l-1 < \nu \le l$, $0 < \alpha_1 < \alpha_2 < \cdots < \alpha_m < \nu$, and D^{α} denotes the Caputo fractional derivative of order α defined by (2.2). We assume that the continuous function F satisfies a uniform Lipschitz condition with Lipschitz constant L in all its arguments except for the first on a suitable domain. For details about the existence, uniqueness and continuous dependence of the solution to this problem refer to [44].

4 Multiple-step adaptive pseudospectral method for FIVPs

In this section we derive the multiple-step adaptive pseudospectral method and apply it to solve the multi-order FIVP (3.1)–(3.2). To solve this problem, we first replace it with a sequence of problems in subintervals. Then these problems are step by step reduced to systems of algebraic equations using collocation based on the ShLG collocation points.

4.1 Problem replacement

Let $h > 0$ be the step-size. Consider the subintervals $I_k = [(k-1)h, kh]$, $k = 1, 2, \ldots$ and let $y_k(x)$ be the solution of the FIVP in the subinterval I_k. The FIVP (3.1)–(3.2) can be replaced with the following sequence of FIVPs on subintervals I_k:

$$D^{\nu}y_{(k)}(x) = F\left(x, y_k(x), D^{\alpha_1}y_{(k)}(x), \ldots, D^{\alpha_m}y_{(k)}(x)\right), \quad x \in I_k, \quad k = 1, 2, \ldots \qquad (4.1)$$

$$y_k^{(r)}\left((k-1)h\right) = y_{k-1}^{(r)}\left((k-1)h\right), \quad r = 0, 1, \ldots, l-1, \qquad (4.2)$$

where the notation $y_{(k)}$ means that the function y is considered up to the k^{th} subinterval, i.e.,

$$y_{(k)}(x) = \begin{cases} y_1(x), & x \in I_1; \\ y_2(x), & x \in I_2; \\ \vdots & \\ y_k(x), & x \in I_k. \end{cases}$$

Note that the reason for introducing this notation is the non-locality of the Caputo differential operator. It is important to mention that, according to (4.2), the initial conditions for step k (except for the first step where the initial conditions are available in (3.2)) are determined based on the solution obtained earlier at step $k-1$. We choose to solve this sequence of problems via Legendre–Gauss adaptive pseudospectral method because of its high accuracy in large domain calculations.

4.2 Piecewise polynomial interpolation

Consider the ShLG collocation points $(k-1)h < x_{k1} < \cdots < x_{k,N-1} < kh$ on the k^{th} subinterval I_k, $k = 1, 2, \ldots$, obtained using the relation (2.5). Obviously,

$$x_{kj} = \frac{h}{2}(z_j + 2k - 1), \quad j = 1, 2, \ldots, N-1. \qquad (4.3)$$

Also, consider two additional noncollocated points $x_{k0} = (k-1)h$ and $x_{kN} = kh$. Let us consider the space of polynomials of degree at most N on the subinterval I_k as

$$\mathcal{P}_N(I_k) = \operatorname{span}\{L_{k0}(x), L_{k1}(x), \dots, L_{kN}(x)\},$$

where

$$L_{ki}(x) = \prod_{l=0, l\neq i}^{N} \frac{x - x_{kl}}{x_{ki} - x_{kl}}, \quad i = 0, 1, \dots, N,$$

is a basis of Lagrange polynomials on subinterval I_k that satisfy $L_{ki}(x_{kj}) = \delta_{ij}$ where δ_{ij} is the Kronecker delta function. The $L^2(I_k)$-orthogonal projection $\mathcal{I}_N : L^2(I_k) \to \mathcal{P}_N(I_k)$ is a mapping in a way that for any $y_k \in L^2(I_k)$ we have

$$\langle \mathcal{I}_N(y_k) - y_k, \phi_k \rangle = 0, \quad \forall\, \phi_k \in \mathcal{P}_N(I_k),$$

or equivalently

$$\mathcal{I}_N(y_k)(x) = \sum_{i=0}^{N} y_{ki} L_{ki}(x), \quad x \in I_k, \tag{4.4}$$

where $y_{ki} = y_k(x_{ki})$. Here, it can be easily seen that for $i = 0, 1, \dots, N$ and $k = 1, 2, \dots,$ we have

$$L_{ki}(x) = L_{1i}\left(x - x_{k0}\right), \quad x \in I_k. \tag{4.5}$$

Thus, by utilizing Eq. (4.5) for Eq. (4.4), the approximation of $y_k(x)$ within each subinterval I_k can be restated as

$$y_k(x) \simeq \mathcal{I}_N(y_k)(x) = \sum_{i=0}^{N} y_{ki} L_{1i}\left(x - x_{k0}\right) = \overset{T}{\mathbf{Y}}_k \mathbf{L}_k(x), \quad x \in I_k, \tag{4.6}$$

where $\mathbf{Y}_k$ and $\mathbf{L}_k(x)$ are $(N+1) \times 1$ matrices given by $\mathbf{Y}_k = [y_{k0}, \dots, y_{kN}]^T$ and $\mathbf{L}_k(x) = [L_{10}(x - x_{k0}), \dots, L_{1N}(x - x_{k0})]^T$. It is observed that the series (4.6) includes the Lagrange polynomials associated with the noncollocated points $x_{k0} = (k-1)h$ and $x_{kN} = kh$, i.e., the initial and terminal points of each subinterval. This then allows more accurate initial conditions to be obtained for the sequence of problems (4.1)–(4.2). Moreover, it is seen from (4.6) that in the present multiple-step scheme, it is only needed to produce the basis of Lagrange polynomials $L_{1i}(x)$ at the first step, which reduces the number of arithmetic calculations and storage requirements especially when the number of steps is large. Now consider the interval $[0, T]$ such that for a positive integer K, $\bigcup_{k=1}^{K} I_k = [0, T]$. For $N \geqslant 1$ we introduce the piecewise polynomials space

$$\Psi_{I_k}^N = \{y \in C[0, T] : y_k = y|_{I_k} \in \mathcal{P}_N(I_k)\},$$

which is the space of the continuous functions over $[0, T]$ whose restrictions on each subinterval I_k are polynomials of degree $\leq N$. Then, for any continuous function y in $[0, T]$, the piecewise interpolation polynomial, $\psi_N(y)$, coincides on each subinterval I_k with the interpolating polynomial $\mathcal{I}_N(y)$ of $y_k = y|_{I_k}$ at the ShLG points.

Next, in a typical collocation method the derivatives of the unknown function y_k are approximated by the analytic derivatives of the interpolating polynomial [35, 36]. The polynomials of degree $N - l$, $(\mathcal{I}_N(y_k))^{(l)}$, are called *Legendre–Gauss interpolation derivatives* of y_k [35]. By differentiating (4.6), l times, the ShLG interpolation derivatives of the function y on each subinterval I_k, $k = 1, 2, \dots,$ are obtained as

$$y_k^{(l)}(x) \simeq (\mathcal{I}_N(y_k))^{(l)}(x) = \overset{T}{\mathbf{Y}}_k \mathbf{L}_k^{(l)}(x), \quad x \in I_k, \quad l \geqslant 1, \tag{4.7}$$

where $\mathbf{L}_k^{(l)}(x) = \frac{d^l}{\mathrm{d}x^l} \mathbf{L}_k(x)$.

4.3 Error estimates

In this subsection, we give some estimates for the errors of piecewise Legendre–Gauss interpolation and its integer-order and fractional-order derivatives. We recall that denoted by $y^{(l)}$ the distributional derivative of function y of order l, the Sobolev space of integer order $r \geq 0$ in the interval (a, b) is defined by [35]

$$H^r(a, b) = \{y \in L^2(a, b) : \text{for } 0 \leq l \leq r, y^{(l)} \in L^2(a, b)\}. \tag{4.8}$$

The associated norm is

$$\|y\|_{H^r(a,b)} = \left(\sum_{l=0}^{r} \int_a^b |y^{(l)}(x)|^2 dx \right)^{1/2} = \left(\sum_{l=0}^{r} \|y^{(l)}\|_{L^2(a,b)}^2 \right)^{1/2}. \tag{4.9}$$

According to the error bounds (5.4.33) and (5.4.34) of [35], the following error estimates hold.

Theorem 1. *Let $y_k \in H^r(I_k)$ with integers $1 \leq r \leq N+1$, then*

$$\left\| y_k - \mathcal{I}_N(y_k) \right\|_{L^2(I_k)} \leq C h^r N^{-r} \|y_k^{(r)}\|_{L^2(I_k)}, \tag{4.10}$$

and for $1 \leq l \leq r$, we have

$$\left\| y_k^{(l)} - (\mathcal{I}_N(y_k))^{(l)} \right\|_{L^2(I_k)} \leq C h^{r-l} N^{2l-r-\frac{1}{2}} \|y_k^{(r)}\|_{L^2(I_k)}, \tag{4.11}$$

where C is a generic positive constant that depends on r, but which is independent of h, N and any function.

Proof. Consult [40]. □

Similar results hold for the piecewise interpolation error $y-\psi_N(y)$ in the norms of the Sobolev spaces (see Theorem 1 of [40]). In the next theorem, we shall give an estimate in the maximum norm.

Theorem 2. *Let $y_k \in H^r(I_k)$ with integers $1 \le r \le N+1$, then for $0 \le l \le r$ we have*

$$\left\| y_k^{(l)}(x) - (\mathcal{I}_N(y_k))^{(l)}(x) \right\|_{L^\infty(I_k)} \le C h^{r-l-\frac{1}{2}} N^{2l-r+\frac{3}{2}} \|y_k^{(r)}\|_{L^2(I_k)}. \tag{4.12}$$

Proof. For any $f \in H^1(I_k)$ with $f(0) = 0$, using Hölder's inequality one has

$$\begin{aligned} |f(x)|^2 = \int_0^x \frac{\mathrm{d}}{\mathrm{d}t}(f^2(t))\,\mathrm{d}t &\le 2\,\|f\|_{L^2(I_k)} \left\| \frac{\mathrm{d}f}{\mathrm{d}t} \right\|_{L^2(I_k)} \\ &\le h^{-1}\,\|f\|^2_{L^2(I_k)} + h \left\| \frac{\mathrm{d}f}{\mathrm{d}t} \right\|^2_{L^2(I_k)}. \end{aligned}$$

For $x \in I_k$, this inequality, along with (4.10) and (4.11), leads to

$$\begin{aligned} \left| y_k^{(l)}(x) - (\mathcal{I}_N(y_k))^{(l)}(x) \right|^2 \le & h^{-1} \left\| y_k^{(l)} - (\mathcal{I}_N(y_k))^{(l)} \right\|^2_{L^2(I_k)} \\ & + h \left\| y_k^{(l+1)} - (\mathcal{I}_N(y_k))^{(l+1)} \right\|^2_{L^2(I_k)} \\ \le & C h^{2r-2l-1} N^{4l-2r+3} \|y_k^{(r)}\|^2_{L^2(I_k)}, \end{aligned}$$

and the proof is completed. □

The following theorem gives an estimate for the piecewise interpolation fractional derivatives error, $D^\alpha y - D^\alpha \psi_N(y)$, in the maximum norm. In what follows, similarly to the definition of $y_{(k)}$ in Subsection 4.1, the notation ψ_N^k means that the piecewise interpolation is considered up to the k^{th} subinterval I_k.

Theorem 3. *Let $\alpha > 0$ and $n = [\alpha]+1$. Suppose $y_k \in H^r(I_k)$, $k = 1, 2, \ldots$, for $1 \le n \le r$, then*

$$\begin{aligned} &\left\| D^\alpha y_{(k)}(x) - D^\alpha \psi_N^k(y)(x) \right\|_{L^\infty(I_k)} \\ &\le C_\alpha h^{r-\alpha-\frac{1}{2}} N^{2n-r+\frac{3}{2}} \sum_{s=1}^{k} \|y_s^{(r)}\|_{L^2(I_s)}, \end{aligned} \tag{4.13}$$

where C_α depends on α, but which is independent of h, N and any function.

Proof. Let $x \in I_k$, then, using the definition of Caputo fractional derivative (2.2) and by triangular and Hölder's inequalities, we obtain

$$\begin{aligned} &\left| D^\alpha y_{(k)}(x) - D^\alpha \psi_N^k(y)(x) \right| \\ &= \frac{1}{\Gamma(n-\alpha)} \left| \sum_{s=1}^{k-1} \int_{I_s} \frac{y_s^{(n)}(t) - (\mathcal{I}_N(y_s))^{(n)}(t)}{(x-t)^{\alpha-n+1}}\,\mathrm{d}t \right. \\ &\quad \left. + \int_{(k-1)h}^{x} \frac{y_k^{(n)}(t) - (\mathcal{I}_N(y_k))^{(n)}(t)}{(x-t)^{\alpha-n+1}}\,\mathrm{d}t \right| \\ &\le \frac{1}{\Gamma(n-\alpha)} \left(\sum_{s=1}^{k-1} \int_{I_s} \frac{\left| y_s^{(n)}(t) - (\mathcal{I}_N(y_s))^{(n)}(t) \right|}{(x-t)^{\alpha-n+1}}\,\mathrm{d}t \right. \\ &\quad \left. + \int_{(k-1)h}^{x} \frac{\left| y_k^{(n)}(t) - (\mathcal{I}_N(y_k))^{(n)}(t) \right|}{(x-t)^{\alpha-n+1}}\,\mathrm{d}t \right) \\ &\le \frac{1}{\Gamma(n-\alpha)} \\ &\quad \left(\sum_{s=1}^{k} \left\| y_s^{(n)}(x) - (\mathcal{I}_N(y_s))^{(n)}(x) \right\|_{L^\infty(I_s)} \left\| (x-t)^{n-\alpha-1} \right\|_{L^1(I_s)} \right) \\ &\le \frac{1}{(n-\alpha)\Gamma(n-\alpha)} h^{n-\alpha} \sum_{s=1}^{k} \left\| y_s^{(n)}(x) - (\mathcal{I}_N(y_s))^{(n)}(x) \right\|_{L^\infty(I_s)} \\ &\le \frac{1}{\Gamma(n-\alpha+1)} C\, h^{r-\alpha-\frac{1}{2}} N^{2n-r+\frac{3}{2}} \sum_{s=1}^{k} \|y_s^{(r)}\|_{L^2(I_s)}, \end{aligned}$$

where Theorem 2 has been used for the last inequality. □

Remark 1. The estimates (4.10)–(4.13) indicate that the errors decay as $h \to 0$. Meanwhile, for fixed h, the errors decay as N and r increase. So, the smoother the exact solutions, the smaller the numerical errors. Furthermore, one can deduce that for increasing the computational accuracy, increasing the mode N suitably is more effective than decreasing the step-size h. However, a step-size $h \le 1$ would provide more rapid convergence rate.

Remark 2. If $y^{(r)} \in L^\infty(0, kh)$ and $2n+2 \le r \le N+1$, then for $k \geqslant 1$, Theorem 3 implies

$$\begin{aligned} &\left\| D^\alpha y_{(k)}(x) - D^\alpha \psi_N^k(y)(x) \right\|_{L^\infty(0,kh)} \\ &\le C_\alpha h^{r-\alpha-\frac{1}{2}} N^{2n-r+\frac{3}{2}} \sum_{s=1}^{k} \sqrt{h} \|y_s^{(r)}\|_{L^\infty(I_s)} \\ &\le C_\alpha k\, h^{r-\alpha} N^{2n-r+\frac{3}{2}} \|y^{(r)}\|_{L^\infty(0,kh)}, \end{aligned} \tag{4.14}$$

which means that the point-wise error of piecewise interpolation fractional derivatives accumulates linearly in terms of k.

4.4 Numerical evaluation of Caputo fractional derivatives

As in a typical pseudospectral method [35], it is crucial to evaluate the values of $D^\alpha y(x)$ at the ShLG collocation points x_{kj}, $k = 1, 2, \dots,$ $j = 1, \dots, N-1$, using an accurate and stable numerical method. In this subsection, we present a stable scheme for approximating the values of $D^\alpha y(x_{kj})$. Our technique is based on the direct usage of the Caputo definition. From the definition of the Caputo fractional derivative (2.2) and using Eqs. (4.6) and (4.7), we have

$$\begin{aligned} D^\alpha y(x_{kj}) &= D^\alpha y_{(k)}(x_{kj}) \approx D^\alpha \psi_N^k(y)(x_{kj}) \\ &= \frac{1}{\Gamma(n-\alpha)} \left(\sum_{s=1}^{k-1} \int_{I_s} \frac{\mathbf{Y}_s^T \mathbf{L}_s^{(n)}(t)}{(x_{kj}-t)^{\alpha-n+1}} \,\mathrm{d}t + \int_{x_{k0}}^{x_{kj}} \frac{\mathbf{Y}_k^T \mathbf{L}_k^{(n)}(t)}{(x_{kj}-t)^{\alpha-n+1}} \,\mathrm{d}t \right). \end{aligned} \tag{4.15}$$

To calculate the integrals on the right-hand side of Eq. (4.15), the Gaussian quadrature rule (2.6) is used in each subinterval. Therefore,

$$\int_{I_s} \frac{\mathbf{Y}_s^T \mathbf{L}_s^{(n)}(t)}{(x_{kj}-t)^{\alpha-n+1}} \,\mathrm{d}t \approx \frac{h}{2} \sum_{i=1}^{N-1} w_i \frac{\mathbf{Y}_s^T \mathbf{L}_s^{(n)}(x_{si})}{(x_{kj}-x_{si})^{\alpha-n+1}} := H_{s,n,j}, \tag{4.16}$$

$$s = 1, \dots, k-1.$$

Moreover, in order to use the Gaussian integration formula in subinterval I_k for the last integral in Eq. (4.15), the change of variables $\tau = \frac{h}{x_{1j}}(t - x_{k0}) + x_{k0}$ should be applied, which yields

$$\begin{aligned} \int_{x_{k0}}^{x_{kj}} \frac{\mathbf{Y}_k^T \mathbf{L}_k^{(n)}(t)}{(x_{kj}-t)^{\alpha-n+1}} \,\mathrm{d}t &= \frac{x_{1j}}{h} \int_{x_{k0}}^{x_{kN}} \frac{\mathbf{Y}_k^T \mathbf{L}_k^{(n)} \left(\frac{x_{1j}}{h}(\tau - x_{k0}) + x_{k0} \right)}{\left(x_{1j} - \frac{x_{1j}}{h}(\tau - x_{k0}) \right)^{\alpha-n+1}} \,\mathrm{d}\tau \\ &\approx \frac{x_{1j}}{2} \sum_{i=1}^{N-1} w_i \frac{\mathbf{Y}_k^T \mathbf{L}_k^{(n)} \left(\frac{x_{1j}x_{1i}}{h} + x_{k0} \right)}{\left(x_{1j} - \frac{x_{1j}x_{1i}}{h} \right)^{\alpha-n+1}} \\ &:= \widetilde{H}_{k,n,j}. \end{aligned} \tag{4.17}$$

Substituting (4.16) and (4.17) into (4.15), results

$$D^\alpha y(x_{kj}) \approx D^\alpha \psi_N^k(y)(x_{kj}) \approx \frac{1}{\Gamma(n-\alpha)} \left(\sum_{s=1}^{k-1} H_{s,n,j} + \widetilde{H}_{k,n,j} \right). \tag{4.18}$$

Unfortunately, the numerical evaluation (4.18) can be problematic in finite arithmetic. In fact, it is not stable when α changes between two consecutive positive integers. This problem arises from the fact that the coefficients $\left(x_{1j} - \frac{x_{1j}x_{1i}}{h} \right)^{n-\alpha-1}$ in (4.17) become large when α increases. We remedy this deficiency by utilizing integration by parts. By integrating by parts, Eq. (4.17) reads

$$\int_{x_{k0}}^{x_{kj}} \frac{\mathbf{Y}_k^T \mathbf{L}_k^{(n)}(t)}{(x_{kj}-t)^{\alpha-n+1}} \,\mathrm{d}t \approx \frac{1}{n-\alpha} \left(x_{1j}^{n-\alpha} \mathbf{Y}_k^T \mathbf{L}_k^{(n)}(x_{k0}) + \widetilde{H}_{k,n+1,j} \right). \tag{4.19}$$

Finally, substituting (4.16) and (4.19) into (4.15) we arrive at the following approximation:

$$\begin{aligned} D^\alpha y(x_{kj}) &\approx D^\alpha \psi_N^k(y)(x_{kj}) \\ &\approx \frac{1}{\Gamma(n-\alpha)} \sum_{s=1}^{k-1} H_{s,n,j} \\ &\quad + \frac{1}{\Gamma(n-\alpha+1)} \left(x_{1j}^{n-\alpha} \mathbf{Y}_k^T \mathbf{L}_k^{(n)}(x_{k0}) + \widetilde{H}_{k,n+1,j} \right) \\ &:= \mathrm{d}_{k,j}^\alpha, \quad k = 1, 2 \dots; \; j = 1, \dots, N-1. \end{aligned} \tag{4.20}$$

The stability and more accuracy of the approximation (4.20) compared to that of the approximation (4.18) is illustrated in Fig. 1, where we plotted the maximum absolute errors $E_\alpha = \max \left\{ \left| D^\alpha y(x_{kj}) - \mathrm{d}_{k,j}^\alpha \right|, \; k = 1, 2; \; j = 1, \dots, N-1 \right\}$ obtained by (4.18) and (4.20) for the function $y(x) = x^{5/2}$, $x \in [0, 1]$ for $0 < \alpha < 2$ and different values of N. As we can see, the approximate values obtained by using (4.18) become quite inaccurate when α goes to 1 or 2. In contrast, (4.20) leads to much more accurate approximations of $D^\alpha y(x_{kj})$. In addition, Fig. 1 illustrates the convergence of the approximation (4.20). Indeed, the convergence of the approximation (4.20) is a consequence of Theorems 1–3 and the high accuracy of the Gaussian quadrature rule provided that the function y is sufficiently smooth.

4.5 The multiple-step collocation method

Consider the problem replacement as explained in Subsection 4.1. Collocating the k^{th} FIVP in subinterval I_k, $k = 1, 2, \dots$ given by Eq. (4.1) at the ShLG collocation points x_{kj} for $j = 1, 2, \dots, N-l+1$ using Eqs. (4.6) and (4.20), we obtain the collocation condition

$$\mathrm{d}_{k,j}^\nu - F\left(x_{kj}, y_{kj}, \mathrm{d}_{k,j}^{\alpha_1}, \dots, \mathrm{d}_{k,j}^{\alpha_m} \right) = 0, \quad j = 1, 2, \dots, N-l+1, \tag{4.21}$$

Moreover, the initial conditions of the k^{th} FIVP in subinterval I_k given by Eq. (4.2), are approximated using Eqs. (4.6) and (4.7) as

$$\mathbf{Y}_k^T \mathbf{L}_k^{(r)}(x_{k0}) - \mathbf{Y}_{k-1}^T \mathbf{L}_{k-1}^{(r)}(x_{k0}) = 0, \quad r = 0, 1, \dots, l-1. \tag{4.22}$$

We note that the vector $\mathbf{Y}_{k-1}$ is obtained earlier at step $k-1$. Also, the initial conditions of the first step are given

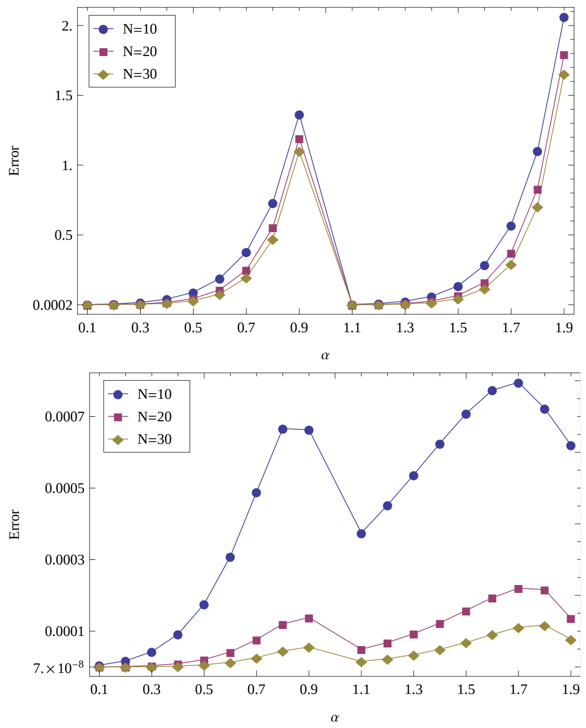

Fig. 1: Maximum absolute errors E_α for the function $y(x) = x^{5/2}$ by using (4.18) (left) and by using (4.20) (right).

by (3.2). At step k, $k = 1, 2, \dots$, Eq. (4.21) together with Eq. (4.22) give a system of equations with $N + 1$ set of algebraic equations, which can be solved with one of the known methods to find the unknowns y_{kj} of the vector $\mathbf{Y}_k$. Consequently, the unknown function $y_k(x)$ in Eq. (4.6) can be calculated at the k^{th} step, which is indeed the approximate solution of the FIVP (3.1)–(3.2) on the subinterval $[(k-1)h, kh)$.

Remark 3. As the error estimates and the numerical evaluations in subsections 4.3 and 4.4 promise us, the interpolation error and the error in its Caputo derivative in the proposed multi-step LG pseudospectral method decays as fast as the global smoothness of the underlying solution permits. Specially, since the function F in (3.1) is continuously differentiable, then in step k, $D^{\nu}\psi_N^k(y)(x) - F\left(x, \mathcal{I}_N(y_k)(x), D^{\alpha_1}\psi_N^k(y)(x), \dots, D^{\alpha_m}\psi_N^k(y)(x)\right)$ goes to $D^{\nu}y_{(k)}(x) - F\left(x, y_k(x), D^{\alpha_1}y_{(k)}(x), \dots, D^{\alpha_m}y_{(k)}(x)\right)$ as $k, N \to \infty$ and the point-wise error of the numerical solution accumulates linearly in terms of the number of steps k. This convergence property will also be discussed in the next section via several test examples.

5 Numerical examples

In this section, we solve several linear and nonlinear FIVPs with the method based on preceding sections, to support our theoretical discussion. Comparisons of the results obtained with those obtained by other methods and also with the exact solutions reveal that the present method is very effective, convenient and accurate. All computations were performed on a 2.2 GHz Core i5 machine with 4 GB RAM running MATHEMATICA 10.0 (Wolfram Research, Champaign, Illinois). All CPU times shown include the total time required to solve the sequence of algebraic systems on all steps. Note that the CPU time is highly dependent on the number of steps and the number of collocation points in each step.

Example 1. As the first example, we consider the following linear FIVP [28]

$$D^{\alpha}y(x) + y(x) = 0, \quad 0 < \alpha \le 2, \tag{5.1}$$

$$y(0) = 1, \quad y'(0) = 0. \tag{5.2}$$

The condition $y'(0) = 0$ is only for $1 < \alpha \le 2$. The exact solution of this problem is given by $y(x) = E_\alpha(-x^\alpha)$, where $E_\alpha(z) = \sum_{k=0}^{\infty} \frac{z^k}{\Gamma(\alpha k+1)}$ is the Mittag-Leffler function [1] of order α.

This problem was solved by applying the technique described in Section 4. In Table 1, the computational times are given and the absolute errors for $\alpha = 0.85$, $x \in [0, 5]$ and different values of h and N are compared with the errors obtained in [19] by using the oprational matrix of fractional derivatives of Legendre polynomials. From Table 1, we see that in the present multiple-step pseudospectral method the accuracy can be improved with both decreasing the step-size and increasing the number of collocation points in subintervals. With regard to CPU time, it is seen that the computation time is growing as h decreases and N increases. This is due to the non-local nature of Caputo derivative and increment in the size of the algebraic systems to be solved. Table 2 compares the maximum absolute errors in the interval $[0, 1]$ for $h = 0.25$, $N = 30$ and different values of α with the errors obtained in [19], [20] and [33] which indicates that the present method is more accurate. Also, the numerical results for $y(x)$, $x \in [0, 10]$ with $h = 1$, $N = 30$ and $\alpha = 0.75, 0.85, 0.95, 0.99$, and 1 together with the exact solutions $E_\alpha(-x^\alpha)$ are plotted in Fig. 2, which shows that the numerical results are in high agreement with the exact ones.

For $1 < \alpha \le 2$, Fig. 3 and Fig. 4 illustrate the numerical solutions by multiple-step pseudospectral method for

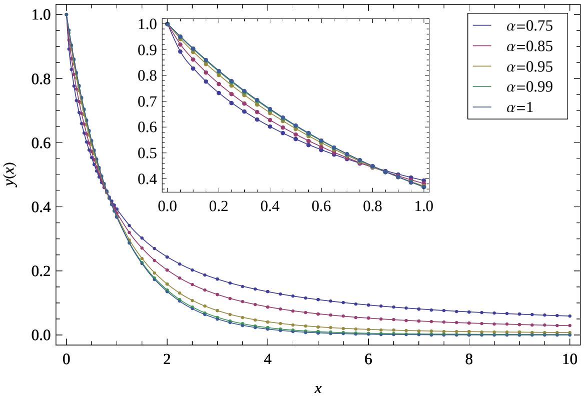

Fig. 2: Comparison of $y(x)$ for $h = 1$, $N = 30$ and $0 < \alpha \leq 1$ with exact solutions for Example 1. Points are discrete approximations

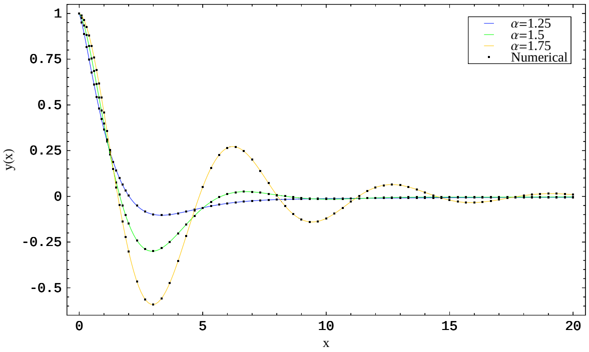

Fig. 3: Comparison of $y(x)$ for $h = 1$, $N = 30$ and $\alpha = 1.25, 1.5, 1.75$ with exact solutions for Example 1.

$x \in [0, 20]$, $h = 1$, $N = 30$ and the exact ones $E_\alpha(-x^\alpha)$ for $\alpha = 1.25, 1.5, 1.75, 1.85, 1.95, 1.99$ and 2. Obviously the numerical results highly agree with the exact ones. For $\alpha = 1$, the exact solution is given as $y(x) = \exp(-x)$, and for $\alpha = 2$, the exact solution is given as $y(x) = \cos(x)$. It is seen in Figs. 2–4 that as α approaches 1 or 2, the numerical solution converges to the analytical solutions, i.e., in the limit, the solution of the fractional differential equations approaches to that of the integer-order differential equations.

Author of Ref. [14] solved this problem using cubic B-spline wavelet collocation method and plotted the numerical results for $y(x)$ for various values of α. Comparison of Figs. 2–4 of this paper with figures 1–3 in [14] reveals that the new multiple-step pseudospectral method approximates the solution more accurately. This example also shows the efficiency of the presented method for large domain calculations.

Example 2. Our second example covers the Bagley–Torvik equation that governs the motion of a rigid plate immersed in a Newtonian fluid.

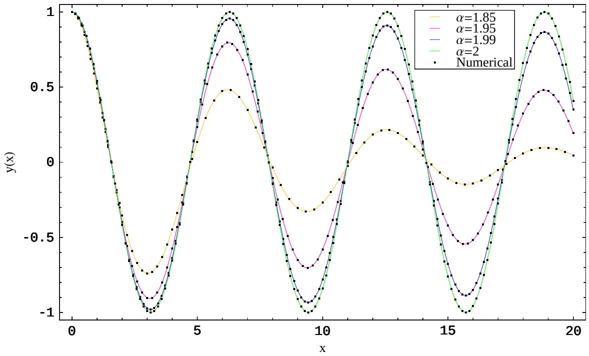

Fig. 4: Comparison of $y(x)$ for $h = 1$, $N = 30$ and $\alpha = 1.85, 1.95, 1.99, 2$ with exact solutions for Example 1.

$$AD^2 y(x) + BD^{\frac{3}{2}} y(x) + Cy(x) = f(x). \tag{5.3}$$

Following [1], [6] and [8], we consider the case $A = 1$, $B = C = \frac{1}{2}$ and $f(x) = 8v(x) - 8v(x-1)$, where $v(x)$ is the Heaviside function, with the following homogeneous initial conditions:

$$y(0) = 0, \quad y'(0) = 0. \tag{5.4}$$

An analytical solution of Equation (5.3) with homogeneous initial conditions (5.4) has been given by Podlubny [1].

$$y(x) = \int_0^x G_3(x-t) f(t)\,\mathrm{d}t,$$

$$G_3(x) = \frac{1}{A} \sum_{k=0}^{\infty} \frac{(-1)^k}{k!} \left(\frac{C}{A}\right)^k x^{2k+1} E^{(k)}_{\frac{1}{2}, 2+\frac{3k}{2}} \left(-\frac{B}{A}\sqrt{x}\right),$$

$$E^{(k)}_{\lambda,\mu}(z) = \frac{\mathrm{d}^k}{\mathrm{d}z^k} E_{\lambda,\mu}(z) = \sum_{j=0}^{\infty} \frac{(j+k)!z^j}{j!\Gamma(\lambda j + \lambda k + \mu)},$$

$$k = 0, 1, 2, \ldots,$$

where $E_{\lambda,\mu}$ is the Mittag-Leffler function in two parameters and the G_3 three-term Green's function. However, in practice, these equations can not be evaluated easily for different functions $f(x)$ and also for large values of x.

Here, we solve this problem using the present multiple-step pseudospectral method with the step-sizes $h = 1$ and 0.5, and different values of N along the interval [0, 30]. Because of propagation of the error due to solving the problem step by step, the convergence at $x = T$ is representative of the convergence on the entire interval $[0, T]$. The errors at $x = 30$ obtained using the present method together with the computation times are given in Table 3. The errors are computed with respect to the

Table 1: Absolute errors for $\alpha = 0.85$ in the interval $[0, 5]$ for Example 1.

	$h = 1$ (5 steps)		$h = 0.25$ (20 steps)		
	$N = 20$	$N = 30$	$N = 20$	$N = 30$	Method [19]
CPU time (s)	7.78	54.75	90.22	312.63	
x					
0.1	$1.7{\times}10^{-4}$	$8.5{\times}10^{-5}$	5.8×10^{-5}	$2.5{\times}10^{-5}$	$8.0{\times}10^{-4}$
0.2	$1.2{\times}10^{-4}$	$8.4{\times}10^{-5}$	3.4×10^{-5}	$1.8{\times}10^{-5}$	$1.2{\times}10^{-3}$
0.3	$1.3{\times}10^{-4}$	$6.6{\times}10^{-5}$	2.6×10^{-5}	$1.2{\times}10^{-5}$	$6.6{\times}10^{-4}$
0.4	$1.3{\times}10^{-4}$	$5.5{\times}10^{-5}$	2.2×10^{-5}	$9.8{\times}10^{-6}$	$8.0{\times}10^{-4}$
0.5	$7.3{\times}10^{-5}$	$4.7{\times}10^{-5}$	1.8×10^{-5}	$8.2{\times}10^{-6}$	$7.5{\times}10^{-4}$
0.6	$8.9{\times}10^{-5}$	$4.1{\times}10^{-5}$	1.3×10^{-5}	$6.3{\times}10^{-6}$	$5.9{\times}10^{-4}$
0.7	$7.4{\times}10^{-5}$	$3.4{\times}10^{-5}$	1.1×10^{-5}	$5.5{\times}10^{-6}$	$7.6{\times}10^{-4}$
0.8	$4.3{\times}10^{-5}$	$2.9{\times}10^{-5}$	7.7×10^{-6}	$3.9{\times}10^{-6}$	$1.8{\times}10^{-4}$
0.9	$3.9{\times}10^{-5}$	$1.9{\times}10^{-5}$	7.3×10^{-6}	$3.6{\times}10^{-6}$	$6.2{\times}10^{-4}$
1.0	$4.1{\times}10^{-5}$	$1.9{\times}10^{-5}$	6.3×10^{-6}	$3.1{\times}10^{-6}$	$1.5{\times}10^{-4}$
2.0	$1.2{\times}10^{-5}$	$5.8{\times}10^{-6}$	5.3×10^{-7}	$5.0{\times}10^{-7}$	–
3.0	$4.8{\times}10^{-6}$	$2.4{\times}10^{-6}$	2.9×10^{-7}	$2.4{\times}10^{-8}$	–
4.0	$2.3{\times}10^{-6}$	$1.2{\times}10^{-6}$	3.2×10^{-7}	$7.0{\times}10^{-8}$	–
5.0	$1.4{\times}10^{-6}$	$7.0{\times}10^{-7}$	2.3×10^{-7}	$5.9{\times}10^{-8}$	–

Table 2: Comparison of maximum absolute errors in $[0, 1]$ for Example 1.

α	Present method	Method [19]	Method [20]	Method [33]
0.2	$3.5{\times}10^{-2}$	$7.4{\times}10^{-1}$	$5.3{\times}10^{-3}$	7.64×10^{-2}
0.4	$6.7{\times}10^{-3}$	$7.3{\times}10^{-1}$	$1.9{\times}10^{-3}$	–
0.6	$6.9{\times}10^{-4}$	$6.7{\times}10^{-3}$	$1.5{\times}10^{-3}$	–
0.8	$1.5{\times}10^{-4}$	$1.2{\times}10^{-3}$	$1.0{\times}10^{-3}$	1.40×10^{-3}
1.2	$7.1{\times}10^{-5}$	$4.5{\times}10^{-3}$	$2.5{\times}10^{-3}$	3.29×10^{-3}
1.4	$2.3{\times}10^{-5}$	$1.3{\times}10^{-3}$	$2.4{\times}10^{-3}$	–
1.6	$1.9{\times}10^{-5}$	$3.1{\times}10^{-4}$	–	–
1.8	$1.8{\times}10^{-5}$	$6.1{\times}10^{-5}$	–	4.29×10^{-5}

value $y(30) = -0.5115451206$ obtained by the analytical solution. In this problem it is seen that obtaining an accurate solution requires significantly more CPU time because, here, we have considered larger domain.

Fig. 5 shows the numerical solution obtained using the present method with $h = 1$, $N = 30$ and the excellent agreement of our multiple-step pseudospectral solution with the analytical solution. A numerical solution of Bagley–Torvik equation (5.3)–(5.4) along the interval $[0, 30]$ has been proposed in [6]. Later this problem was solved in [8] using the Adomian decomposition method. Note that some deviations of solutions obtained in [6] and [8] from that of Podlubny [1] are exist (see [6] Fig. 3 and [8] Fig. 2). This demonstrates the superior accuracy of the present solution.

From Fig. 5 it can be concluded that the solution of this Bagley-Torvik equation oscillates and goes to zero as $x \to \infty$. In Fig. 6 we have plotted the numerical solution obtained using the present method with $h = 1$, $N = 20$ on the interval $[0, 100]$, which confirms the above mentioned tendency. It should be noted that it is very difficult and time consuming to evaluate the analytical solution by Podlubny [1] over the interval $[0, 100]$. In addition, the truncated ADM series solution given in [8] up to 200 terms diverges after a certain time (see Fig. 7). Again, it is observed that the present method is capable of giving very accurate results even for large domain calculations.

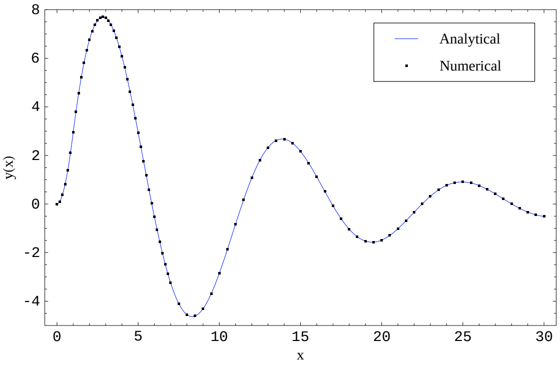

Fig. 5: Comparison of the present numerical solution and the analytical solution for Example 2.

Example 3. Consider the following nonlinear multi-order FIVP

$$aD^2y(x) + bD^{\alpha_2}y(x) + cD^{\alpha_1}y(x) + ey^3(x) = 2ax + \frac{2bx^{3-\alpha_2}}{\Gamma(4-\alpha_2)} + \frac{2cx^{3-\alpha_1}}{\Gamma(4-\alpha_1)} + \frac{ex^9}{27}, \quad 0 < \alpha_1 < \alpha_2 \le 1, \tag{5.5}$$

Table 3: Absolute errors $|y(30) - \psi_N(y)(30)|$ using the present method for Example 2.

N	$h = 1$ (30 steps)	CPU time (s)	$h = 0.5$ (60 steps)	CPU time (s)
5	5.19×10^{-4}	0.36	2.06×10^{-4}	1.58
10	5.47×10^{-5}	7.97	2.16×10^{-5}	35.94
20	6.30×10^{-6}	264.52	3.10×10^{-6}	731.16
30	1.81×10^{-6}	578.23	7.09×10^{-7}	1378.59

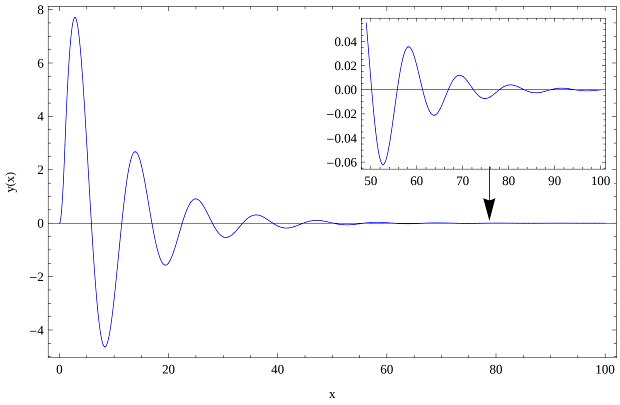

Fig. 6: The Graph of Bagley-Torvik equation using the present method with $h = 1$ and $N = 20$ on the interval $[0, 100]$.

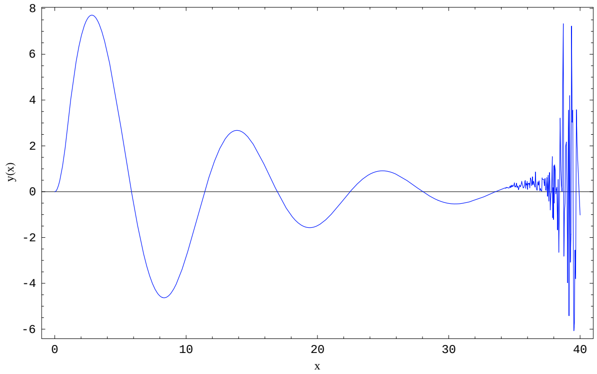

Fig. 7: The Adomian Decomposition Method series solution of Bagley-Torvik equation. The divergence after a certain time is apparent.

$$y(0) = 0, \quad y'(0) = 0, \tag{5.6}$$

where a, b, c and e are real numbers. The exact solution of this problem is given by $y(x) = \frac{1}{3}x^3$.

This problem was solved in [16] using Adomian decomposition method (ADM) and a proposed numerical method (PNM) in the interval $[0, 2]$. Here, we solve this problem using the present multiple-step pseudospectral method in the interval $[0, 5]$ for ($a = 1$, $b = 2$, $c = 1/2$, $e = 1$, $\alpha_1 = 0.00196$, $\alpha_2 = 0.07621$) and ($a = 1$, $b = 0.1$, $c = 0.2$, $e = 0.3$, $\alpha_1 = \frac{\sqrt{5}}{5}$, $\alpha_2 = \frac{\sqrt{2}}{2}$).

Table 4 shows a comparison between the present solution and solutions obtained in [16] when ($a = 1$, $b = 2$, $c = 1/2$, $e = 1$, $\alpha_1 = 0.00196$, $\alpha_2 = 0.07621$). Also, Table 5 shows a comparison between the present solution and solutions obtained in [16] when ($a = 1$, $b = 0.1$, $c = 0.2$, $e = 0.3$, $\alpha_1 = \frac{\sqrt{5}}{5}$, $\alpha_2 = \frac{\sqrt{2}}{2}$). From these two tables it is seen that the present method is much more accurate. Moreover, the convergence of the presented method is apparent.

Example 4. Consider the following nonlinear multi-order FIVP,

$$D^{\alpha}y(x) + D^{\beta}y(x)D^{\gamma}y(x) + y^2(x) = x^6 + \frac{6}{\Gamma(4-\alpha)}x^{3-\alpha} + \frac{36}{\Gamma(4-\gamma)\Gamma(4-\beta)}x^{6-\beta-\gamma}, \tag{5.7}$$

$$y(0) = y'(0) = y''(0) = 0, \tag{5.8}$$

where $\alpha \in (2, 3)$, $\gamma \in (1, 2)$ and $\beta \in (0, 1)$. The exact solution to this problem is $y(x) = x^3$.

In Table 6, we give the computational time and we compare the absolute errors obtained by the present multiple-step pseudospectral method for $h = 1$ and $N = 40$ with the shifted Chebyshev collocation method presented in [21], with different values of α, γ and β. Also in Table 7 we compare the maximum absolute errors in the interval $[0, 1]$, obtained using the present method and the shifted Jacobi collocation method [22], at $\alpha = 2.5$, $\gamma = 1.5$, $\beta = 0.9$ with various choices of h and N. In the case of $\alpha = 2.7$, $\gamma = 1.7$, $\beta = 0.7$, the approximate solution in the interval $[0, 6]$, obtained by the present method for $h = 1$ and $N = 30$ is shown in Fig. 8 to make it easier to compare with the analytic solution.

Example 5. Consider the nonlinear multi-order FIVP with oscillatory behavior,

$$D^{\alpha}y(x) + D^{\beta}y(x) + e^{-y^2(x)} = \sin(2x), \tag{5.9}$$

$$y(0) = 0, \quad y'(0) = -1, \tag{5.10}$$

where $\alpha \in (1, 2]$ and $\beta \in (0, 1]$. For $\alpha = 2$ and $\beta = 1$ a numeric solution can be obtained by direct numerical inte-

Table 4: Comparison of absolute errors for ($a = 1$, $b = 2$, $c = 1/2$, $e = 1$, $\alpha_1 = 0.00196$, $\alpha_2 = 0.07621$) and $h = 1$ for Example 3.

CPU time (s)	0.52	15.71	118.32		
x	$N = 10$	$N = 20$	$N = 30$	PNM [16]	ADM [16]
0.2	2.6×10^{-10}	1.6×10^{-11}	3.3×10^{-12}	3.93409×10^{-5}	9.12455×10^{-11}
0.4	8.0×10^{-9}	4.9×10^{-10}	9.9×10^{-11}	1.53545×10^{-4}	4.08994×10^{-8}
0.6	5.8×10^{-8}	3.6×10^{-9}	7.2×10^{-10}	3.30564×10^{-4}	1.46310×10^{-6}
0.8	2.3×10^{-7}	1.4×10^{-8}	2.9×10^{-9}	5.52441×10^{-4}	1.89999×10^{-5}
1.0	6.8×10^{-7}	4.2×10^{-8}	8.5×10^{-9}	7.97757×10^{-4}	1.50218×10^{-4}
1.2	6.2×10^{-7}	3.7×10^{-8}	7.6×10^{-9}	1.04618×10^{-3}	9.63935×10^{-4}
1.4	4.5×10^{-7}	2.9×10^{-8}	5.9×10^{-9}	1.29004×10^{-3}	5.97725×10^{-3}
1.6	3.4×10^{-7}	2.3×10^{-8}	4.9×10^{-9}	1.56444×10^{-3}	3.82246×10^{-2}
1.8	4.5×10^{-7}	3.2×10^{-8}	6.5×10^{-9}	2.00641×10^{-3}	2.55500×10^{-1}
2.0	9.5×10^{-7}	6.1×10^{-8}	1.3×10^{-8}	2.89864×10^{-3}	1.83461×10^{0}
3.0	3.1×10^{-7}	1.4×10^{-8}	2.7×10^{-9}	–	–
4.0	4.9×10^{-6}	7.5×10^{-9}	2.0×10^{-9}	–	–
5.0	3.8×10^{-5}	8.4×10^{-7}	6.6×10^{-9}	–	–

Table 5: Comparison of absolute errors for ($a = 1$, $b = 0.1$, $c = 0.2$, $e = 0.3$, $\alpha_1 = \frac{\sqrt{5}}{5}$, $\alpha_2 = \frac{\sqrt{2}}{2}$) and $h = 1$ for Example 3.

CPU time (s)	0.53	15.59	118.73		
x	$N = 10$	$N = 20$	$N = 30$	PNM [16]	ADM [16]
0.2	6.4×10^{-9}	9.1×10^{-10}	3.0×10^{-10}	3.95794×10^{-5}	4.41567×10^{-11}
0.4	1.3×10^{-7}	1.8×10^{-8}	6.1×10^{-9}	1.57803×10^{-4}	6.65814×10^{-9}
0.6	7.7×10^{-7}	1.1×10^{-7}	3.5×10^{-8}	3.52193×10^{-4}	1.26983×10^{-7}
0.8	2.7×10^{-6}	3.7×10^{-7}	1.2×10^{-7}	6.13120×10^{-4}	1.05072×10^{-6}
1.0	7.1×10^{-6}	9.8×10^{-7}	3.2×10^{-7}	8.68269×10^{-4}	5.74351×10^{-6}
1.2	9.5×10^{-6}	1.3×10^{-6}	4.2×10^{-7}	6.86241×10^{-4}	2.64200×10^{-5}
1.4	1.2×10^{-5}	1.6×10^{-6}	5.4×10^{-7}	1.84769×10^{-3}	1.20987×10^{-4}
1.6	1.5×10^{-5}	2.2×10^{-6}	7.1×10^{-7}	1.34530×10^{-2}	5.96191×10^{-4}
1.8	2.1×10^{-5}	2.9×10^{-6}	9.7×10^{-7}	5.35383×10^{-2}	3.18350×10^{-3}
2.0	2.9×10^{-5}	4.1×10^{-6}	1.3×10^{-6}	1.68659×10^{-1}	1.83619×10^{-2}
3.0	1.6×10^{-5}	2.2×10^{-6}	6.9×10^{-7}	–	–
4.0	6.4×10^{-7}	3.4×10^{-7}	1.1×10^{-7}	–	–
5.0	1.6×10^{-5}	2.2×10^{-6}	7.0×10^{-7}	–	–

Table 6: Comparison of absolute errors for Example 4.

	$\alpha = 2.1, \beta = 0.1, \gamma = 1.1$		$\alpha = 2.5, \beta = 0.99, \gamma = 1.99$	
x	Present method	Method [21]	Present method	Method [21]
	CPU time: 94.67 s		CPU time: 97.21 s	
0	1.9×10^{-20}	4.44×10^{-16}	2.4×10^{-18}	4.44×10^{-16}
0.2	4.3×10^{-13}	3.79×10^{-8}	5.6×10^{-10}	1.01×10^{-6}
0.4	1.4×10^{-11}	3.07×10^{-8}	2.4×10^{-8}	2.57×10^{-6}
0.6	3.3×10^{-10}	4.77×10^{-8}	2.0×10^{-7}	4.45×10^{-6}
0.8	2.5×10^{-9}	6.73×10^{-8}	8.4×10^{-7}	6.28×10^{-6}
1.0	1.1×10^{-8}	7.78×10^{-8}	2.3×10^{-6}	7.60×10^{-6}
1.2	1.0×10^{-8}	7.23×10^{-8}	3.2×10^{-6}	8.11×10^{-6}
1.4	2.3×10^{-8}	4.70×10^{-8}	3.9×10^{-6}	7.80×10^{-6}
1.6	2.3×10^{-8}	1.68×10^{-8}	5.1×10^{-6}	6.82×10^{-6}
1.8	6.7×10^{-9}	1.77×10^{-8}	7.1×10^{-6}	5.43×10^{-6}
2.0	1.2×10^{-8}	3.44×10^{-9}	8.9×10^{-6}	3.73×10^{-6}

gration in MATHEMATICA, which we compare with the solution we get by our multiple-step pseudospectral scheme. In this case, the maximum absolute error on the interval $[0, 80]$ for $h = 1$, $N = 10$ is obtained as 1.37×10^{-8}. Fig. 9 shows the oscillatory behavior of the solution to this case.

Table 7: Comparison of maximum absolute errors on the interval [0, 1] for $\alpha = 2.5$, $\beta = 0.9$, $\gamma = 1.5$ for Example 4.

	Present method				
N	$h = 1$	CPU time (s)	$h = 0.5$	CPU time (s)	Method [22]
4	1.5×10^{-3}	0.02	2.9×10^{-4}	0.16	1.27×10^{-3}
8	2.6×10^{-4}	0.05	2.6×10^{-5}	0.26	3.47×10^{-4}
16	4.8×10^{-5}	1.77	8.2×10^{-6}	4.91	8.98×10^{-5}
24	1.8×10^{-5}	7.55	3.7×10^{-6}	21.98	3.15×10^{-5}

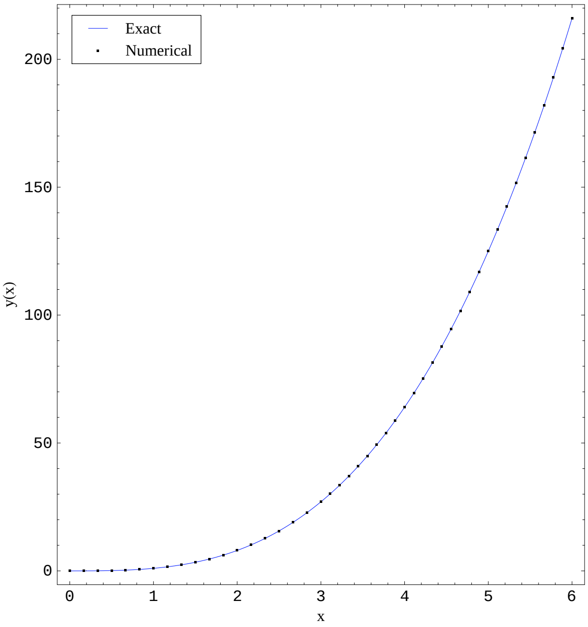

Fig. 8: Comparison of $y(x)$ with $h = 1$, $N = 30$ for $\alpha = 2.7$, $\beta = 0.7$, $\gamma = 1.7$ for Example 4.

The exact solutions for the values of $\alpha \in (1, 2)$ and $\beta \in (0, 1)$ are not exist, and we remark that there is not a built-in command in MATHEMATICA for solving fractional differential equations. Therefore, to show the convergence of the present method for this problem over an interval $[0, T]$, we suggest the following practical and easy-to-use convergence index: As Remark 1 suggests us, we first set $h = 1$ and then we solve the problem for different values of $N \leq \bar{N}$ until the following convergence criteria is satisfied,

$$e_N = \left|\psi_N(y)(T) - \psi_{N-1}(y)(T)\right| < \epsilon,$$

where $\bar{N}$ and ϵ are user defined values and may be vary from one problem to another. If the specified convergence tolerance ϵ has not been satisfied yet, then we decrease the step-size h and solve the problem as above. It is important to note that, due to the exponential convergence of pseudospectral methods in a subinterval where the solution is smooth and because $h \leq 1$, there is no need to use very large number of collocation points in subintervals. In this example we set $T = 50$, $\epsilon = 10^{-6}$ and we limit N by setting $\bar{N} = 30$.

Table 8 displays the values of e_N and $\psi_N(y)(50)$ for $h = 1$ (50 steps) and various values of N, α and β. The CPU times are also changed from 2 seconds for $N = 5$ to 1250 seconds for $N = 25$. This table demonstrates the accuracy and convergence of the present multiple-step scheme in large-domain calculations. Also, Figs. 10–12 show the approximate solutions for this problem with the values of α and β given in Table 8. These figures illustrate the different oscillatory behavior of the solutions to this problem for different values of α and β. Duan et al. [17] treat a similar FIVP with the right hand side function equal to 1, which does not have oscillatory behavior, and solved it by the Rach-Adomian-Meyers modified decomposition method only over the interval [0, 3].

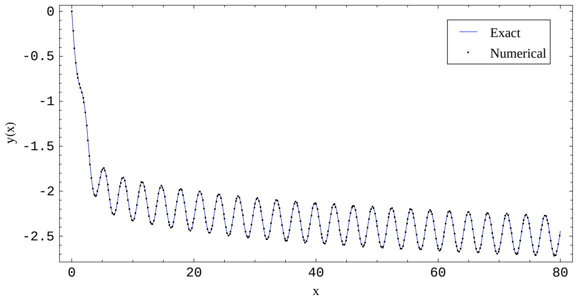

Fig. 9: Comparison of $y(x)$ with $h = 1$, $N = 10$ for $\alpha = 2$ and $\beta = 1$ for Example 5.

Example 6. Finally, to show that the proposed method is also suited for systems of FIVPs, we consider the fractional Lorenz system [45],

$$\begin{cases} D^{\alpha}y_1(x) = \sigma(y_2(x) - y_1(x)) \\ D^{\beta}y_2(x) = Ry_1(x) - y_2(x) - y_1(x)y_3(x) \\ D^{\gamma}y_3(x) = y_1(x)y_2(x) + by_3(x) \\ y_1(0) = -15.8, \quad y_2(0) = -17.48, \quad y_3(0) = 35.64, \end{cases} \tag{5.11}$$

where $0 < \alpha, \beta, \gamma \leq 1$ and y_1, y_2 and y_3 are respectively proportional to the convective velocity, the temperature

Table 8: The values of $\psi_N(y)(50)$ and e_N for various values of α and β for Example 5.

	$\alpha = 1.2,\ \beta = 0.8$		$\alpha = 1.5,\ \beta = 0.5$		$\alpha = 1.85,\ \beta = 0.05$	
N	$\psi_N(y)(50)$	e_N	$\psi_N(y)(50)$	e_N	$\psi_N(y)(50)$	e_N
5	-10.227454	3.92×10^{-3}	-1.931422	1.38×10^{-3}	-0.715699	1.10×10^{-3}
10	-10.225751	1.01×10^{-5}	-1.930962	1.89×10^{-5}	-0.717137	9.58×10^{-5}
15	-10.225533	6.12×10^{-6}	-1.930930	2.90×10^{-6}	-0.717343	2.23×10^{-5}
20	-10.225392	2.19×10^{-6}	-1.930924	7.43×10^{-7}	-0.717404	8.15×10^{-6}
25	-10.225360	8.10×10^{-7}	–	–	-0.717426	8.35×10^{-7}

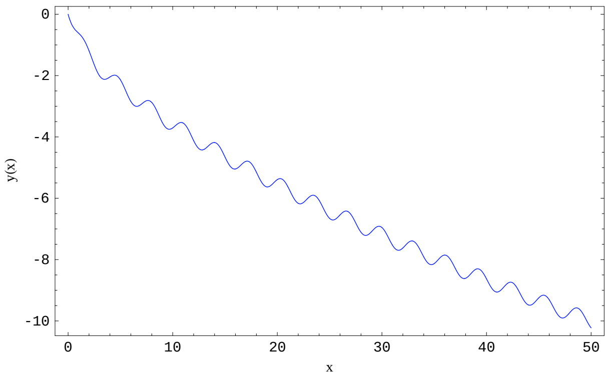

Fig. 10: Computational results of $y(x)$ with $h = 1$, $N = 20$ for $\alpha = 1.2$, $\beta = 0.8$ for Example 5.

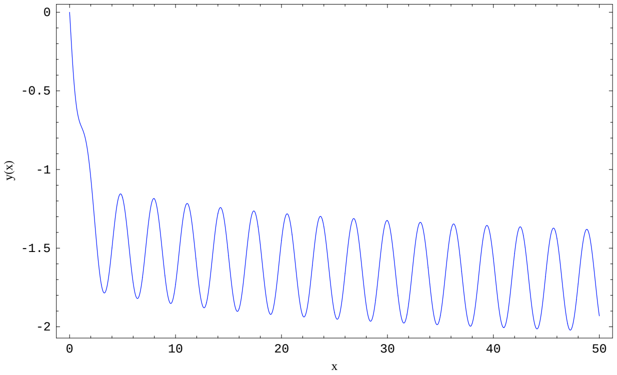

Fig. 11: Computational results of $y(x)$ with $h = 1$, $N = 20$ for $\alpha = 1.5$, $\beta = 0.5$ for Example 5.

difference between descending and ascending flows, and the mean convective heat flow, and σ, b and the so-called bifurcation parameter R are real constants.

As in [45], we set $\sigma = 10$, $b = -\frac{8}{3}$ and $R = 23.5$. The time range studied in this example is $[0, 10]$. The exact solutions for different values of α, β and γ are not available; however, to show the effectiveness of our method, we use the fact that the Caputo fractional order solutions converge to the integer order solutions. Notably, our experiment shows that the solutions of the fractional order Lorenz system are sensitive to the step-size h, i.e., for ensuring the high accuracy, small values of h are required.

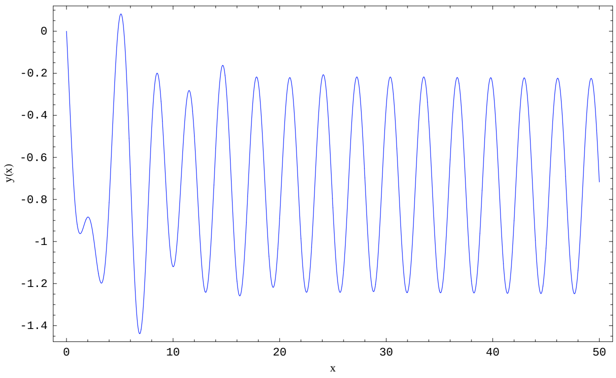

Fig. 12: Computational results of $y(x)$ with $h = 1$, $N = 20$ for $\alpha = 1.85$, $\beta = 0.05$ for Example 5.

Table 9 displays the values of $\psi_N(y)(10)$ for $N = 6$, $h = 0.05$ (200 steps) and various values of α, β and γ. This table demonstrates the convergence of the fractional order solutions to the integer order solution. The CPU times are around 447 seconds.

For the purpose of studying the effectiveness of the fractional order parameters α, β and γ of the Lorenz system, we plot the graphs of y_1, y_2 and y_3 using present method at different cases which are shown in Fig. 13. Therefore, it may be concluded that the solutions of the fractional Lorenz system become almost constant as x increases. Moreover, the solutions remain constant in the whole domain of interest as $\alpha, \beta, \gamma \to 0$, meanwhile they show more oscillatory behavior as $\alpha, \beta, \gamma \to 1$.

6 Conclusions

Fractional differential equations grow more and more popular nowadays to model science and engineering processes. Therefore, finding a reliable and efficient technique to solve them is very important. In this work, an efficient multiple-step pseudospectral method based on the ShLG collocation points has been proposed for numerically solving the multi-order FIVPs. This method is easy to be implemented for linear and nonlinear problems. We converted

Table 9: The values of $\psi_6(y)(10)$ for $h = 0.05$ and various values of (α, β, γ) for Example 6.

	$(0.95, 0.95, 0.95)$	$(0.99, 0.99, 0.99)$	$(0.9999, 0.9999, 0.9999)$	$(1, 1, 1)$
$\psi_6(y_1)(10)$	7.72990806	5.16268791	5.21692823	5.22054356
$\psi_6(y_2)(10)$	7.74327347	4.22467454	4.08500765	4.07467005
$\psi_6(y_3)(10)$	22.47923256	21.46426815	21.54603815	21.57004284

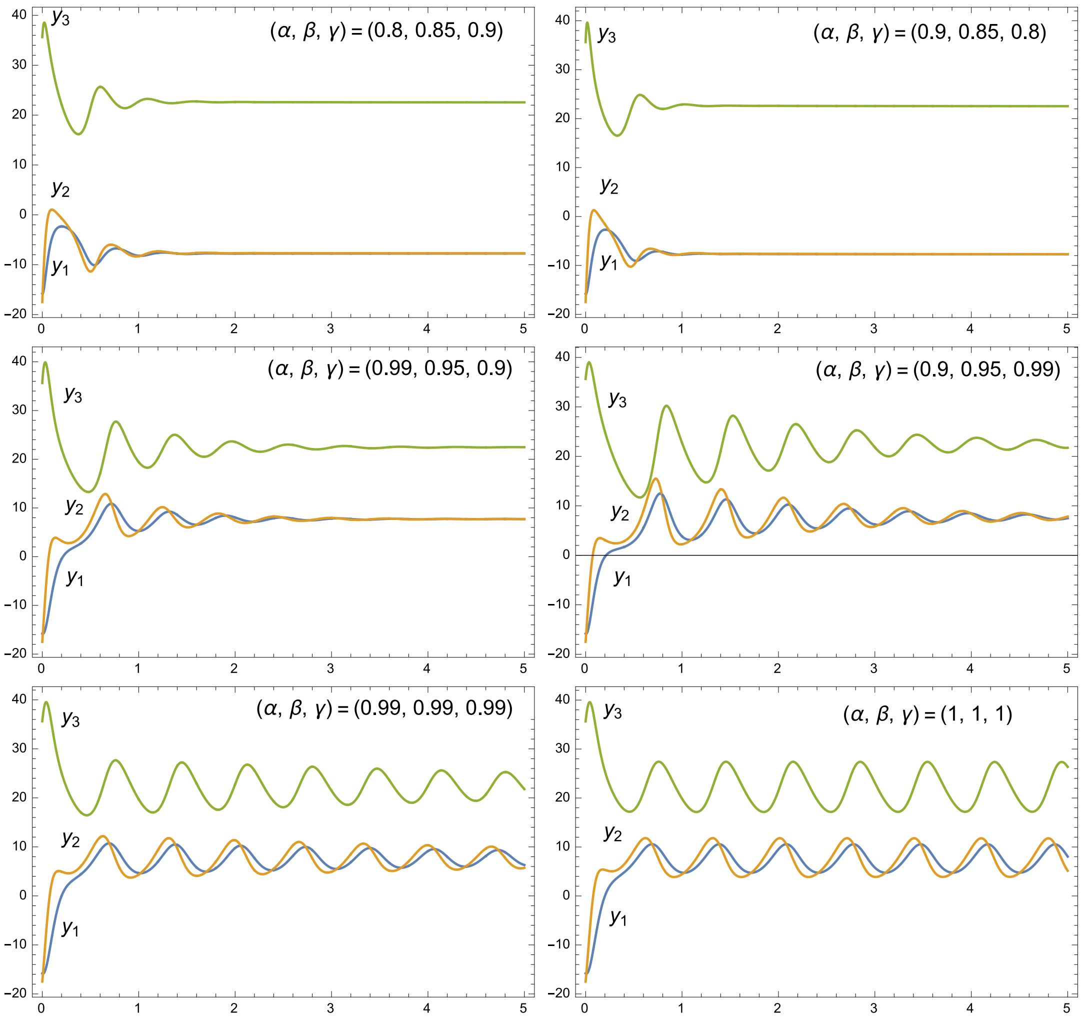

Fig. 13: Computational results for Example 6 with $h = 0.1$ and $N = 10$.

the original FIVP to a sequence of FIVPs in subintervals and solved them, step by step, using collocation, where the initial conditions of each step were obtained from the solution approximated earlier at its previous step. An accurate and stable scheme has been introduced for approximating the values of fractional derivatives at the ShLG collocation points. The numerical results demonstrated the spectral accuracy and convergence of the proposed method. It was shown that the accuracy can be improved either by decreasing the step-size or by increasing the number of collocation points in subintervals. Moreover, this method is valid for large-domain calculations and also for solutions having oscillatory behavior. The achieved results are compared with the exact solutions and with the solutions obtained by some other numerical methods, which demonstrate the validity and superior accuracy of the proposed method.

References

[1] Podlubny I. *Fractional Differential Equations: An Introduction to Fractional Derivatives, Fractional Differential Equations, to Methods of their Solution and Some of their Applications*. Academic Press, New York, 1999.

[2] Kilbas AA, Srivastava HM, Trujillo JJ. *Theory and Applications of Fractional Differential Equations*. San Diego, Elsevier, 2006.

[3] Diethelm K. *The Analysis of Fractional Differential Equations: An Application-Oriented Exposition Using Differential Operators of Caputo Type*. Berlin Heidelberg, Springer, 2010.

[4] Das S. *Functional Fractional Calculus for System Identification and Controls*. New York, Springer, 2008.

[5] Mainardi F. *Fractional calculus: some basic problems in continuum and statistical mechanics, Fractals and Fractional Calculus in Continuum Mechanics*, Springer-Verlag, New York, 1997. pp. 291–348.

[6] Trinks C, Ruge P. Treatment of dynamic systems with fractional derivatives without evaluating memory-integrals. *Computational Mechanics* 2002; **29**: 471–476.

[7] Bagley RL, Torvik PJ. On the appearance of the fractional derivative in the behavior of real materials. *Journal of Applied Mechanics* 1984; 51(2): 294–298.

[8] Saha Ray S, Bera RK. Analytical solution of the Bagley Torvik equation by Adomian decomposition method. *Applied Mathematics and Computation* 2005; 168: 398–410.

[9] Baleanu D. About fractional quantization and fractional variational principles. *Communication in Nonlinear Science and Numerical Simulation* 2009; 14(6): 2520–2523.

[10] Tenreiro-Machado J. Fractional generalization of memristor and higher order elements. *Communication in Nonlinear Science and Numerical Simulation* 2013; 18(2): 264–275.

[11] Moaddy K, Hashim I, Momani S. Non-standard finite difference schemes for solving fractional-order Rössler chaotic and hyperchaotic systems. *Computers and Mathematics with Applications* 2011; 62: 1068–1074.

[12] Li X, Xu C. A space-time spectral method for the time fractional diffusion equation. *SIAM Journal of Numerical Analysis* 2009; 47(3): 2108–2131.

[13] Pedas A, Tamme E. Spline collocation methods for linear multi-term fractional differential equations. *Journal of Computational and Applied Mathematics* 2011; 236: 167–176.

[14] Li X. Numerical solution of fractional differential equations using cubic B-spline wavelet collocation method. *Communication in Nonlinear Science and Numerical Simulation* 2012; 17(10): 3934–3946.

[15] Ford NJ, Connolly AJ. Systems-based decomposition schemes for the approximate solution of multi-term fractional differential equations. *Journal of Computational and Applied Mathematics* 2009; 229: 382–391.

[16] El-Sayed AMA, El-Kalla IL, Ziada EAA. Analytical and numerical solutions of multi-term nonlinear fractional orders differential equations. *Applied Numerical Mathematics* 2010; 60: 788–797.

[17] Duan JS, Chaolu T, Rach R. Solutions of the initial value problem for nonlinear fractional ordinary differential equations by the Rach-Adomian-Meyers modified decomposition method. *Applied Mathematics and Computation* 2012; 218(17): 8370–8392.

[18] He J.H, Wu G.C, Austin F. The variational iteration method which should be followed. *Nonlinear Science Letters A* 2010; 1(1): 1–30.

[19] Saadatmandi A, Dehghan M. A new operational matrix for solving fractional-order differential equations. *Computers and Mathematic with Application* 2010; 59: 1326–1336.

[20] Lakestani M, Dehghan M, Irandoust-Pakchin S. The construction of operational matrix of fractional derivatives using B-spline functions. *Communications in Nonlinear Science and Numerical Simulation* 2012; 17: 1149–1162.

[21] Doha EH, Bhrawy AH, Ezz-Eldien SS. Efficient Chebyshev spectral methods for solving multi-term fractional orders differential equations. *Applied Mathematical Modelling* 2011; 35: 5662–5672.

[22] Doha EH, Bhrawy AH, Ezz-Eldien SS. A new Jacobi operational matrix: An application for solving fractional differential equations. *Applied Mathematical Modelling* 2012; 36(10): 4931–4943.

[23] Li X. Operational method for solving fractional differential equations using cubic B-spline approximation. *International Journal of Computer Mathematics* 2014; doi: 10.1080/00207160.2014.884792.

[24] Maleknejad K, Nouri K, Torkzadeh L. Study on Multi-Order fractional differential equations via Operational Matrix of Hybrid Basis Functions. *Bulletin of Iranian Mathematical Society* 2017; 43(2): 307–318.

[25] Bolandtalat A, Babolian E, Jafari H. Numerical solutions of multi-order fractional differential equations by Boubaker Polynomials. *Open physics* 2016; 14: 226–230.

[26] Zurigat M, Momani S, Alawneh A. The multistage homotopy analysis method: application to a biochemical reaction model of fractional order. *International Journal of Computer Mathematics* 2013; 91(5): 1030–1040.

[27] Kumar D, Sharma RP. Numerical approximation of Newell-Whitehead-Segel equation of fractional order. *Nonlinear Engineering: Modeling and Application* 2016; 5(2): 81-86.

[28] Kumar P, Agrawal OP. An approximate method for numerical solution of fractional differential equations. *Signal Processing* 2006; 86: 2602–2610.

[29] Diethelm K. An algorithm for the numerical solution of differential equations of fractional order. *Electronic Transactions on Numerical Analysis* 1997; 5: 1–6.

[30] Esmaeili S, Garrappa R. A pseudo-spectral scheme for the approximate solution of a time-fractional diffusion equation. *International Journal of Computer Mathematics* 2014; doi: 10.1080/00207160.2014.915962.

[31] Maleki M, Hashim I, Tavassoli Kajani M, Abbasbandy S. An adaptive pseudospectral method for fractional order boundary value problems. *Abstract and Applied Analysis* Volume 2012, Article ID 381708, doi:10.1155/2012/381708.

[32] Kazem S, Abbasbandy S, Kumar S. Fractional-order Legendre functions for solving fractional-order differential equations. *Applied Mathematical Modelling* 2013; 37(7): 5498–5510.

[33] Rad JA, Kazem S, Shaban M, Parand K, Yildirim A. Numerical solution of fractional differential equations with a Tau method based on Legendre and Bernstein polynomials. *Mathematical Methods in the Applied Sciences* 2014; 37: 329–342.

[34] Baffet D, Hesthaven JS. A Kernel Compression Scheme for Fractional Differential Equations. *SIAM Journal of Numerical analysis.* 2017; 55(2): 496-520.

[35] Canuto C, Hussaini MY, Quarteroni A, Zang TA. *Spectral Methods: Fundamentals in Single Domains*. Springer-Verlag, Berlin, 2006.

[36] Shen J, Tang T, Wang LL. *Spectral Methods: Algorithms, Analysis and Applications*. Springer-Verlag, Berlin, Heidelberg, 2011.

[37] Maleki M, Hashim I, Abbasbandy S. Pseudospectral methods based on nonclassical orthogonal polynomials for solving nonlinear variational problems. *International Journal of Computer Mathematics* 2014; 91(7): 1552–1573.

[38] Guo BY, Yan JP. Legendre–Gauss collocation method for initial value problems of second order ordinary differential equations. *Applied Numerical Mathematics* 2009; 59: 1386–1408.

[39] Guo BY, Wang L. Jacobi approximations in non-uniformly Jacobi-weighted Sobolev spaces. *Journal of Approximation Theory* 2004; 128: 1–41.

[40] Maleki M, Hashim I, Abbasbandy S. Solution of time-varying delay systems using an adaptive collocation method. *Applied Mathematics and Computation* 2012; 219: 1434–1448.

[41] Podlubny I. Geometric and physical interpretation of fractional integration and fractional differentiation. *Fractional Calculus and Applied Analysis* 2002; 5: 367–386.

[42] Caputo M. Linear models of dissipation whose Q is almost frequency independent. *Part II. Journal of the Royal Society of Western Australia* 1967; 13: 529–539.

[43] Diethelm K, Freed AD. *On the solution of nonlinear fractional differential equations used in the modeling of viscoplasticity*. in: F. Keil, W. Mackens, H. Voβ, J. Werther (Eds.), Scientific Computing in Chemical Engineering II-Computational Fluid Dynamics, Reaction Engineering, and Molecular Properties, Springer, Heidelberg, (1999) 217–224.

[44] Diethelm K, Ford NJ. Multi-order fractional differential equations and their numerical solution.*Applied Mathematics and Computation* 2004; 154: 621–640.

[45] Alomari AK, Noorani MSM, Nazar R, Li CP, Homotopy analysis method for solving fractional Lorenz system. *Communication in Nonlinear Science and Numerical Simulation* 2010; 15: 1864–1872.